Proceedings of the 28th IEEE
EMBS Annual International Conference
New York City, USA, Aug 30-Sept 3, 2006

A Dual Band Wireless Power and Data Telemetry for Retinal Prosthesis

Guoxing Wang[1], Wentai Liu[1], Mohanasankar Sivaprakasam[1], Mingcui Zhou[1], James D. Weiland[2], Mark S. Humayun[2]

[1]Department of Electrical Engineering, University of California, Santa Cruz, CA 95064, USA
[2]Department of Ophthalmology, University of Southern California, Los Angeles, CA 90089, USA

Abstract— **Inductive coupling is commonly used for wireless power and data transfer in biomedical telemetry systems. The increasing demand on the performance of medical devices requires high data rate and high power efficiency at the same time. If only one radio frequency carrier is used, it is difficult to achieve both high data rate and high power efficiency due to the competing requirements on carrier frequency and system-*Q* of the power and data transmission. We propose a dual band telemetry system to implement power and data transmission using different frequencies by allocating lower frequency for power transmission and higher frequency for data transmission. However, the magnetic coupling between the power carrier and data carrier will affect the operation of both links. In this paper, this interference is analyzed and design equations are derived, which are used to design coils to maximize the data signal level received at the implant side. A prototype of dual band telemetry for a retinal prosthetic device has been built and experimental results show that both power and data can be transmitted and high data rate can be achieved without compromising the power transmission efficiency.**

I. Introduction

Retinitis Pigmentosa (RP) and Age-Related Macular Degeneration (AMD) are retinal diseases that result in profound vision loss due to degeneration of the light sensing photoreceptor cells. The discovery that direct electrical stimulation of retinal ganglion/bipolar cells creates visual excitation in patients has inspired an electronic prosthetic device capable of bypassing the damaged photoreceptors [1], [2]. Such a device is composed of a camera, power and bi-directional data telemetry links, micro stimulator chip and micro electrode array (Fig. 1). The camera mounted on special glasses captures the image. Both power and image data are wirelessly transmitted to the implant through coupled coil pair(s). Power is also transmitted to the implant from an external coil mounted on the glasses. Large amounts of power and high data rate are required for stimulating a large number of electrodes. For stimulation of 1000 electrodes, it is estimated that a data rate of 1~ 2Mbps and a power of 100 mW are needed.

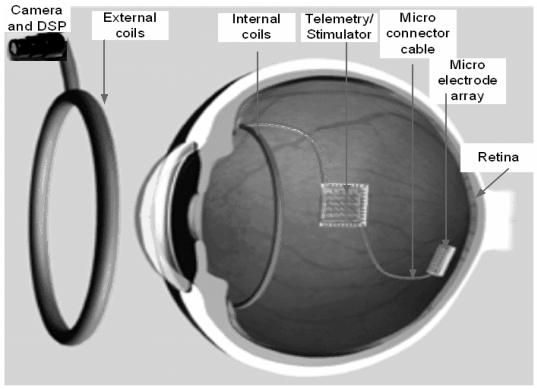

Fig. 1. Conceptual diagram of retinal prosthesis

Traditionally in biomedical telemetry, the power carrier is also used for data transmission [2], [3], [4]. High data rate often requires high carrier frequency and/or low *Q* of the transmission system. However, power transmission generally requires no higher than tens of MHz carrier frequency to well penetrate the tissue [5] and high *Q* to achieve high efficiency, which is directly in contradiction with the requirements of the data transmission.

To accommodate the high data rate while still efficiently providing power, a dual band telemetry link (Fig. 2) is proposed, with one link transmitting power (power link) while the other transmitting data (data link). This system separates the data transmission from the power delivery, by allocating lower frequency (f_{pwr}) for the power and higher frequency (f_{data}) for forward data carriers. High frequency of the data carrier makes it possible to achieve high data rate without compromising the efficiency of power transmission. In this paper, such a dual band power and data telemetry system is presented, with emphasis on how to achieve good signal strength for data transmission through analytical techniques.

II. System Schematic

As shown in Fig. 2, in the power and data transmission system, four coils are employed, L_{1_p}, L_{2_p}, L_{1_d}, and L_{2_d}. The coil pair L_{1_p} and L_{2_p} is for power transmission and the coil pair L_{1_d} and L_{2_d} is for data transmission. Class-E power amplifiers are used to drive the primary side coils. For power transmission, this is due to the high power conversion efficiency that Class-E provides [6], [7]. For data transmission, the Class-E power amplifier is a specially designed phase shift

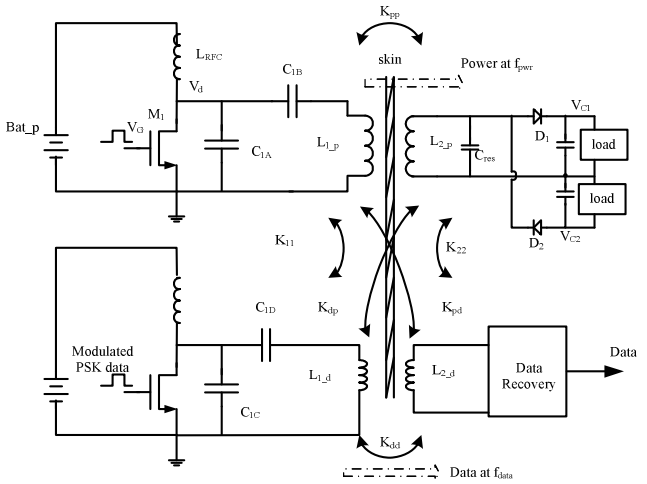

Fig. 2. Simplified schematic of dual band telemetry system.

keying (PSK) modulator proposed by the authors [8]. Interested readers are referred to the references. The power recovery circuits on the secondary side employ a dual diode rectification circuit [9] to achieve dual voltage supply, which is used by stimulator circuits to generate bi-phasic pulses to stimulate the neurons [10].

As shown in Fig. 2, there are six coupling coefficients between the coils. K_{pp} is the main coupling transferring power from L_{1_p} to L_{2_p} and K_{dd} is the main coupling that provides data signal from L_{1_d} to L_{2_d}. K_{pd} is the coupling between the primary power coil and secondary data coil. K_{11} is the coupling coefficient between the primary two coils, L_{1_p} and L_{1_d}. K_{22} is the coupling coefficient between the two secondary coils, L_{2_p} and L_{2_d}. K_{dp} is the coupling between the primary data coil and secondary power coil. The six coupling coefficients affect the circuit design in a non-trivial way. For example, the existence of power coils affects the data link in two ways. One is that the magnetic field generated for power transmission (at frequency f_{pwr}) will generate a noise voltage on the data receiving coil ($L_{2\text{-}d}$). Another one is that the signal strength (at f_{data}) is reduced due to the counteracting magnetic field generated by the power coils. This counteracting magnetic field may reduce the signal strength to an undetectable level if not carefully designed. In this paper, a methodology of designing the data link to achieve large data signal strength under the constraints of power link is presented.

III. Power Link Effect on Data Signal Strength

In the following analysis, ω_{pwr} and ω_{data} represent the angular frequency of the power carrier and data carrier, respectively. Assume the current in L_{1_d} is I_{L1_d} with frequency of ω_{data}, which represents the modulated data signal. I_{L1_d} induces a magnetic field and generates a voltage in series with the $L_{2\text{-}d}$ [11],

$$V_{ind\,2\_d}^{(1)} = I_{L1\_d} \cdot j\omega_{data} K_{dd} \sqrt{L_{1\_d} L_{2\_d}} \tag{1}$$

This is the major signal for data transmission.

Due to the coupling between the primary power coil and primary data coil (K_{11}), the current I_{L1_d} also generates a voltage on L_{1_p},

$$V_{ind\,1\_p} = I_{L1\_d} \cdot j\omega_{data} K_{11} \sqrt{L_{1\_d} L_{1\_p}} \tag{2}$$

This voltage V_{ind1_p} generates a current of $I_{L1\_p}^{(d)}$, where the superscript (d) denotes the current at frequency f_{data} instead of the total current through the power coil which also includes the component at frequency f_{pwr}.

$$I_{L1\_p}^{(d)} = -\frac{V_{ind1\_p}}{Z_{1T\_p}} \approx -\frac{V_{ind1\_p}}{j\omega_{data} L_{1\_p}} \tag{3}$$

The negative sign indicates that the induced current is out of phase with the current I_{L1_d}, which is in accordance with Lenz's Law that the induced current generates a magnetic field to counteract the one that produces it. Z_{1T_p} is the equivalent impedance seen by the induced voltage V_{ind1_p}, which is comprised of L_{1_p}, C_{1A}, C_{1B} and the Class-E switch. Z_{1T_p} can be approximated to the impedance of $L_{1\text{-}p}$ because at data carrier frequency f_{data} ($>>f_{pwr}$), the impedances of C_{1A} and C_{1B} are much smaller than $\omega_{data} \cdot L_{1\_p}$ since C_{1A} and C_{1B} are tuned at frequency f_{pwr} (or very close) and. The Class-E switch M_1 which is in parallel to C_{1A} can be ignored since the impedance will be even smaller if the switch is turned on. In other words, the total impedance is dominated by the coil inductance L_{1_p}, the rest of its loading circuit acts like a short circuit at frequency f_{data}.

Further simplification of (3) using (2) results in (4).

$$I_{L1\_p}^{(d)} = -I_{L1\_d} K_{11} \sqrt{\frac{L_{1\_d}}{L_{1\_p}}} \tag{4}$$

The current $I_{L1\_p}^{(d)}$ in turn generates a voltage on the secondary side data coil,

$$\begin{aligned} V_{ind\,2\_d}^{(2)} &= I_{L1\_p}^{(d)} \cdot j\omega_{data} K_{pd} \sqrt{L_{1\_p} L_{2\_d}} \\ &= -I_{L1\_d} \cdot j\omega_{data} K_{11} K_{pd} \sqrt{L_{1\_d} L_{2\_d}} \end{aligned} \tag{5}$$

Obviously, this induced voltage is out of phase from the voltage in (1). As a result, the strength of the received data signal at the secondary data coil is reduced due to the current in the primary power coil (I_{L1_p}). This shows a destructive signal path from $L_{1\text{-}d}$, $L_{1\text{-}p}$ to $L_{2\text{-}d}$.

Similarly, another signal path from $L_{1\text{-}d}$, $L_{2\text{-}p}$ to $L_{2\text{-}d}$ exists and this path also generates a destructive voltage on the secondary data coil,

$$V_{ind\,2\_d}^{(3)} = -I_{L1\_d} \cdot j\omega_{data} K_{dp} K_{22} \sqrt{L_{1\_d} L_{2\_d}} \tag{6}$$

This equation assumes that at high frequencies (f_{data}), the equivalent impedance loaded on L_{2_p} is negligible compared to the impedance of L_{2_p} itself. The loading impedance includes the resonant capacitance C_{res} and the rectification circuit parallel to it. This assumption is true considering that the resonating capacitor C_{res} in Fig. 2 is tuned to the lower frequency f_{pwr} and acts like a short circuit at frequency f_{data}.

The signal path from L_{1_d}, L_{1_p}, L_{2_p} to L_{2_d} generates a voltage,

$$V_{ind\,2\_d}^{(4)} = I_{L1\_d} \cdot j\omega_{data} K_{11} K_{pp} K_{22} \sqrt{L_{1\_d} L_{2\_d}} \tag{7}$$

And another signal path from L_{1_d}, L_{2_p}, L_{1_p} to L_{2_d} generates a voltage,

$$V_{ind\,2\_d}^{(5)} = I_{L1\_d} \cdot j\omega_{data} K_{dp} K_{pp} K_{pd} \sqrt{L_{1\_d} L_{2\_d}} \tag{8}$$

The total induced voltage (signal strength) is

$$V_{ind\,2\_d} = V_{ind\,2\_d}^{(1)} + V_{ind\,2\_d}^{(2)} + V_{ind\,2\_d}^{(3)} + V_{ind\,2\_d}^{(4)} + V_{ind\,2\_d}^{(5)} \tag{9}$$

$$V_{ind2\_d} = I_{L1\_d} \cdot j\omega_{data}\sqrt{L_{1\_d}L_{2\_d}} \cdot$$
$$(K_{dd} - K_{11}K_{pd} - K_{dp}K_{22} + K_{11}K_{pp}K_{22} + K_{dp}K_{pp}K_{pd}) \quad (10)$$

Equation (10) is a very important result which will serve as the design guideline to maximize the signal strength. As can be seen, the data signal induced on the secondary data coil is a sum of the constructive and destructive paths, represented by the combination of the coupling coefficients. It is important to maximize the total coupling effects.

Circuits shown in Fig. 2 are simulated using SPICE to verify the equation (10). In simulation, the coils and the associated driver circuits for both power and data link are included. The power recovery circuit is also included. The following parameters are chosen: L_{1_d} = 1 µH, L_{2_d} = 100 nH, f_{data} = 20 MHz, I_{L1_d} = 1 A. The signal strength, V_{L2d}, is the voltage of the data carrier (20 MHz) on the secondary data coil L_{2_d}. The results are shown in Table I, where the voltage level is normalized to I_{L1_d}. In the table, case 1 and case 2 represent the coil distance of 15 mm and 7 mm, respectively. As it can be seen, the equation (10) is accurate in predicting the signal strength.

TABLE I SIGNAL STRENGTH CALCULATION AND SIMULATION RESULTS

	K_{pp}	K_{pd}	K_{dp}	K_{dd}	K_{11}	K_{22}	V_{L2d} Signal (f_{data}) (V)	
							equation	simulation
case 1	0.07	0.04	0.04	0.03	0.21	0.25	0.61	0.60
case 2	0.15	0.08	0.08	0.07	0.21	0.25	1.67	1.59

IV. Design of Data Coils

Equation (10) shows that the coupling coefficient between the coils should be carefully chosen. In order to examine the effect of the coupling coefficients on the signal strength, an effective coupling (K_{eff}) is defined from (10):

$$K_{eff} = K_{dd} - K_{11}K_{pd} - K_{dp}K_{22} + K_{11}K_{pp}K_{22} + K_{dp}K_{pp}K_{pd} \quad (11)$$

As can be seen from (10) and (11), if K_{eff} is zero, the received signal will be zero, regardless of the strength of the driving current I_{L1_d}. This means the effective coupling should be far away from zero under all conditions.

The coupling between coils is a function of the geometrical parameters such as coil sizes, shapes and distance between the coils. In retinal prosthesis, it is estimated that the distance between the external coils and the implanted coils varies between 7 mm and 15 mm due to coil movements. The maximum sizes of the implanted coils are limited by the available space. Generally, the power coils are made as large as possible to maximize the coupling. They also occupy most of the available space since it requires more turns than the data coil, to generate a magnetic field strong enough to transmit power into the implant with acceptable efficiency [7]. So the designer is left only with choosing the data coils to maximize the K_{eff}. Therefore, the sizes of the data coils should be chosen to give the right coupling between the coils and maximize the received data signal strength.

In order to calculate K_{eff}, we need to find individual coupling coefficients corresponding to the specific coil parameters. To simplify the coupling coefficient calculations, all the four coils are assumed to be co-axial, as illustrated in Fig. 3. Generally extensive numerical calculation is required to find coupling coefficients between two coils [12]. Instead, simplified equations from [13] are used to calculate the coupling coefficients.

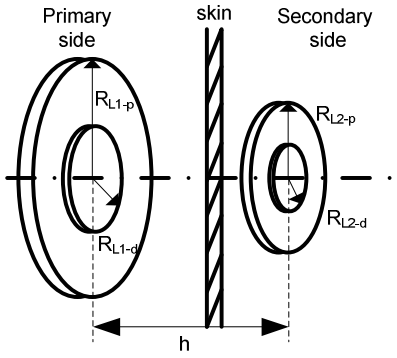

Fig. 3. Illustration of the arrangement of power and data coils.

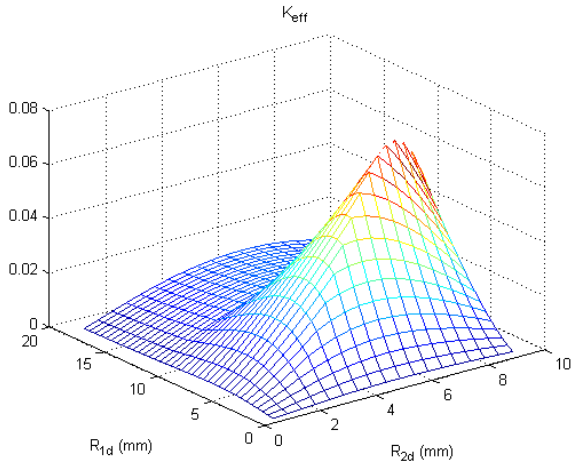

Fig. 4. Effective coupling with different coils sizes (h = 7mm)

Fig. 4 shows the calculated effective coupling when the data coil radii are swept. As shown in Fig. 4, the effective coupling may be zero or even negative. A negative K_{eff} means that the voltage induced on the coil is dominated by the path L_{1_d}, L_{1_p}, L_{2_d} and/or the path L_{1_d}, L_{2_p}, L_{2_d}. K_{eff} should be maximized by choosing appropriate primary and secondary coil radii, and more importantly away from zero to ensure robustness From the plots in Fig. 4, the coil sizes of R_{1_d} = 8.5 mm, R_{2_d} = 6 mm are chosen because they give good coupling for both h = 7 mm and 15 mm cases. It should be emphasized that simply choosing large coil radii to maximize K_{dd} will not work since the corresponding K_{eff} may be low. For example, at distance (h) of 7mm, when R_{1d} and R_{2d} are 8 mm and 11 mm respectively, K_{dd} is 0.12 but K_{eff} is only 0.008.

V. Prototype Results

A dual band wireless power and data telemetry prototype system has been built for retinal prosthesis. The power carrier frequency has been chosen as 1 MHz and the data carrier frequency is 20 MHz. The power coils are optimized given the

geometrical constraints [7]. The data coils are built based on the radii given in the above section. The pictures in Fig. 5 show the data coils together with the power coils. The primary data coil is constructed with four turns, with inductance about 1 µH; the secondary data coil has two turns, with inductance about 100 nH.

Shown in Fig. 6 are the waveforms of the prototype of the dual band telemetry when the primary coils and secondary coils are about 7 mm apart. In the experiment, about 100 mW DC power is received by the implant. The power efficiency is about 30%. In the experiments, no difference in the power transmission has been observed regardless of the existence of the data link. This demonstrates that the power link is relatively independent of the data link and can be designed separately.

When coil distance is 7mm, the power carrier noise (1 MHz) on the secondary data coil is about 300mV peak to peak. The received data signal (20 MHz) is about 100 mV peak to peak. The power carrier noise can be filtered out using a high pass filter. Also from the experiments results, it has been observed that at the maximum coil distance (15 mm), the data signal strength is about 75 mV, which is large enough for the data recovery circuits to detect data.

VI. Conclusions

A dual band telemetry system which implements wireless power transfer using a lower carrier frequency and data transfer using a higher frequency has been proposed in the paper. The interaction between the power transfer and data transfer is analyzed and the resulting equations are used for a design methodology for maximizing the data signal magnitude. A prototype for a retinal prosthetic device is shown to choose the optimal parameters of the coils for data transmission. The experimental results demonstrate that in the dual band telemetry system, data can be transmitted without compromising the power transmission efficiency.

Acknowledgment

The authors would like to acknowledge the financial support provided by National Science Foundation for this work.

References

[1] M. Humayun, E. de Juan Jr., J. Weiland, G. Dagnelie, S. Katona, R.Greenberg, and S. Suzuki., "Pattern electrical stimulation of the human retina," *Vision Res*., vol. 39, pp. 2569-76, 1999.

[2] W. Liu, K. Vichienchom, M. Clements, S. C. DeMarco, C. Hughes, E. McGucken, M. S. Humayun, E. de Juan, J. D. Weiland, R. Greenberg. "A Neuro-Stimulus Chip with Telemetry Unit for Retinal Prosthetic Device," *IEEE J. Solid-State Circuits*. vol. 35, no. 10, pp. 1487-97, Oct. 2000.

[3] M. Ghovanloo, K. Najafi, "A Wideband Frequency-Shift Keying Wireless Link for Inductively Powered Biomedical Implants," *IEEE Transactions on Circuits and Systems I,* pp. 2374-2383, Dec. 2004.

[4] H. McDermott, "An advanced multiple channel cochlear implant," *IEEE Transactions on Biomedical Engineering*, vol. 36, pp. 789 – 797, July 1989.

[5] J. C. Lin, "Computer methods for field intensity predictions," in ch. 9 of *CRC Handbook of Biological Effects of Electromagnetic Fields*, C. Polk and E. Postow, Eds., Boca Raton, FL: CRC Press, 1996.

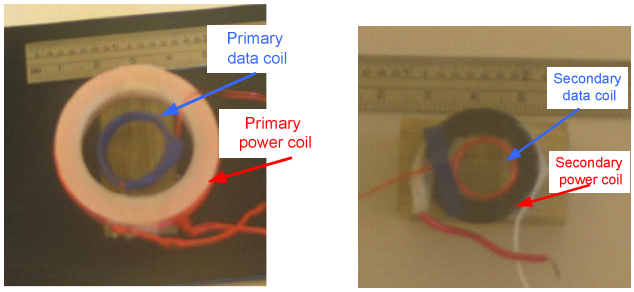

Fig. 5. Coils used in experiments

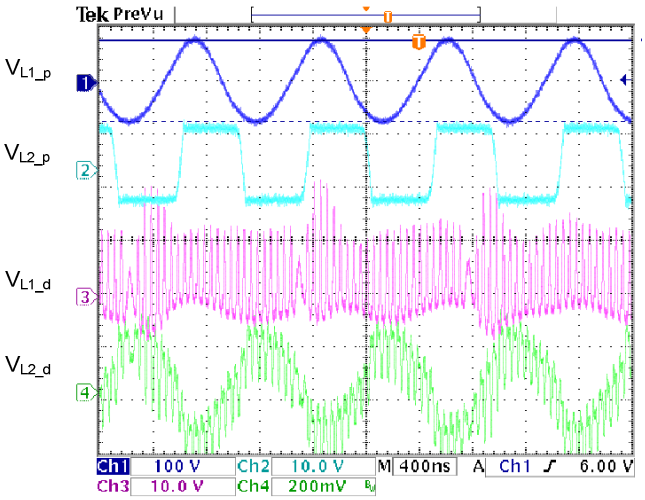

Fig. 6. Typical waveforms of the dual band telemetry

[6] N. O. Sokal and A. D. Sokal, "Class-E- A New Class of High-Efficiency Tuned Single-Ended Switching Power Amplifiers," *IEEE J. Solid-State Circuits*, vol. 10, pp. 168-176, June 1975.

[7] G. A. Kendir, W.Liu, G. Wang, M. Sivaprakasam, R. Bashirullah, M. Humayun, J. Weiland, "An Optimal Design Methodology for Inductive Power Link with Class-E Amplifier," vol. 52, pp. 857 - 866, *IEEE Transactions on Circuits and Systems – I*, May 2005.

[8] G. Wang, W. Liu, M. Sivaprakasam, M. Zhou, M. S. Humayun, and J. D. Weiland, "A Wireless Phase Shift Keying Transmitter with Q-Independent Phase Transition Time," the *27th Annual International Conference of the IEEE Engineering in Medicine and Biology Society*, Shanghai, Sept. 2005.

[9] G. Wang, W. Liu, M. Sivaprakasam, M. S. Humayun, and J. D. Weiland, "Power Supply Topologies for Biphasic Stimulation in Inductively Powered Implants," *IEEE International Symposium on Circuits and Systems*, pp. 2743 – 2746, May 2005.

[10] M. Sivaprakasam, W. Liu, M. S. Humayun, and J. D. Weiland, "A Variable Range Bi-Phasic Current Stimulus Driver Circuitry for an Implantable Retinal Prosthetic Device," vol. 41, pp. 763 – 771, *IEEE Journal of Solid State Circuits*, March 2005.

[11] M. N. O. Sadiku, *Elements of Electromagnetics,* 3rd edition, Oxford University press, 2001.

[12] C.M. Zierhofer, E.S. Hochmair, "High-efficiency coupling-insensitive transcutaneous power and data transmission via an inductive link," *IEEE Trans. Biomed. Eng*., vol. 37, pp. 716-722, 1990.

[13] K. Finkenzeller, *RFID-Handbook,* 2nd Ed., Wiley, Hoboken, NJ, 2003.